RSC Advances

ROYAL SOCIETY OF CHEMISTRY

www.rsc.org/advances

Journal Name

RSCPublishing

COMMUNICATION

The Self-Assembly and Secondary Structure of Peptide Amphiphiles Determine the Membrane Permeation Activity

Cite this: DOI: 10.1039/x0xx00000x

Received ooth January 2012,
Accepted ooth January 2012

DOI: 10.1039/x0xx00000x

www.rsc.org/

Rie Wakabayashi,[*,‡] Yuko Abe,[‡] Noriho Kamiya,[‡,§] and Masahiro Goto[*,‡,§,¶]

Membrane fusogenic peptides have attracted increasing attention because of their unique biofunctions in membrane translocation and viral infection. Here, we designed GALA-related peptides with palmitoyl tails. Our study indicated that the self-assembling propensity and the secondary structure of these peptide amphiphiles greatly influenced the membrane permeability.

Membrane fusion is a protein-mediated event, which is critical in cellular physiology and viral infection.[1–3] Most membrane-active proteins possess fusion peptides. As a common structural feature, these peptides adopt a relatively hydrophobic, amphipathic α -helix when active. Because membrane fusogenic peptides can be useful in bionanotechnology and nanomedicine, not only naturally derived, but de novo designed peptides have been explored extensively.[4]

GALA is an artificial membrane-active peptide designed by Szoka et al.[5,6] The sequence of the GALA peptide (WEAALAEALAEALAEHLAEALAEALEALAA) is composed of repeating sequences of glutamic acid–alanine–leucine–alanine (EALA). The secondary structure of GALA transforms from a random coil to an amphipathic α-helix when the pH is decreased from physiological to slightly acidic conditions (< 6). The formation of a pH-responsive α-helix enables the site-specific activation of the peptide at an intracellular acidic membrane called the endosome. This peptide has significant potential as a functional group for drug delivery via carriers because the structure is believed to enhance the endosomal escape and to deliver efficiently encapsulated drugs into cells.[7–16]

Intensive studies on GALA peptides include the modification of the peptide with different peptide sequences or the conjugation of hydrophobic tails to the terminus. Although GALA-modified peptides with shorter peptide sequences would be synthetically easier, the shorter sequence destabilizes the secondary structure.[5,17] The peptides conjugated with hydrophobic tails, also known as peptide amphiphiles (PAs), form supramolecular assemblies, which can stabilize the secondary structure of the peptides.[18,19] However, the contribution of the self-assembling propensity combined with the secondary structure to the membrane activity has not been explored. In this study, we have synthesized two different PAs with GALA-derived 8 or 14 amino acid sequences and examined how the structural features affect membrane permeating ability.

Scheme 1. Chemical structures of PAs used in this study.

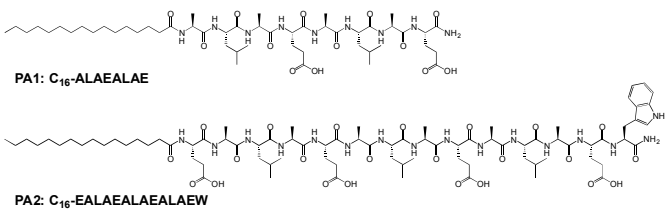

The new PAs have an alanine–leucine–alanine–glutamic acid (ALAE) repeating unit; the palmitoylated peptide sequences are palmitoyl-$(ALAE)_2$ (**PA1**) and palmitoyl-

$E(ALAE)_3W$ (**PA2**) (Scheme 1). In the PA design, the amino acid adjacent to the hydrophobic core plays an important role in the formation of intermolecular hydrogen bonding of PAs.[20–22] The relatively hydrophobic alanine for **PA1** can be expected to assist the formation of β-sheet. The hydrophilic glutamic acid for **PA2** disrupts the intermolecular hydrogen bonding and can lead the peptide to form an α-helix structure, which is found in the original GALA peptide. The secondary structures that **PA1** and **PA2** formed at physiological and acidic pH were confirmed by the circular dichroism (CD) spectroscopy. The characteristic CD spectra for β-sheet structure were observed for **PA1** both at pH 5.5 and 7.5 (Figure 1a). In contrast to **PA1**, **PA2** formed an α-helix with little difference between spectra recorded at pH 5.5 and 7.5 (Figure 1b). We thus succeeded in synthesizing GALA-mimic PAs with different secondary structures. It was reported that short peptides with 4–16 amino acids composed of 1–4 repeating units of EALA, $(EALA)_n$, where n = 1–4, showed no stable secondary structure.[5,17] We assume that the short peptide sequences of **PA1** and **PA2** could form stable secondary structures because the palmitoylation of the amino-terminus decreased the conformational freedom of the molecule.[18,19]

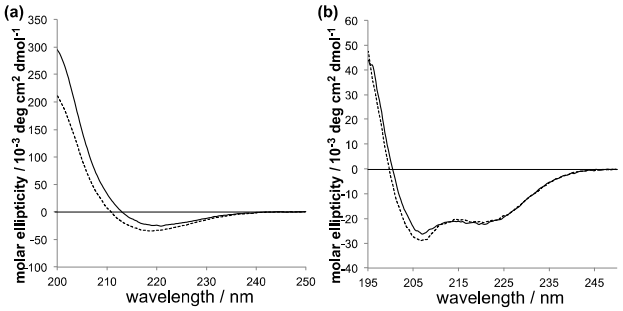

Figure 1. CD spectra of (a) **PA1** and (b) **PA2** at pH 5.5 (dashed) and pH 7.5 (solid).

Because the formation of β-sheet has been found to be important for self-assembly of PAs,[20–22] **PA1** may have higher tendency to assemble than **PA2**. To investigate the self-aggregation propensity of the peptides, the critical micelle concentration (CMC) was determined by using the pyrene solubilization method.[23] The CMC values of **PA1** both at pH 5.5 and 7.5 were lower than those of **PA2** (Figure S2). It is clear that the formation of a β-sheet structure through intramolecular hydrogen bonding is important for self-assembly. Interestingly, **PA1** has a higher CMC at pH 5.5 than pH 7.5 (8 μM for pH 5.5 and 2 μM for pH 7.5), whereas **PA2** has a similar CMC at pH 5.5 and pH 7.5 (12 μM). This result indicated that the aggregation scheme differs between **PA1** and **PA2**; the balance between hydrophilicity and hydrophobicity is important for the β-sheet forming **PA1** by enabling efficient intramolecular hydrogen bonding, whereas the protonation of the glutamate has little influence on aggregation for the α-helix forming **PA2**. It indicates that the main driving force of assembly for **PA2** is the hydrophobic interaction between the palmitoyl tails. Since **PA2** forms amphipathic α-helix both at pH 5.5 and 7.5, the hydrophobic interaction between leucine residues may have an additional contribution to the assembly. Although acylated GALA peptides with fatty acids show lower CMC values under acidic conditions because of the protonation of glutamate side chains,[19] the protonation of shorter peptide sequences of **PA2** may have less influence on aggregation.

The aggregation of PAs was further confirmed by transmission electron microscopy (TEM). Nanofibers with microns lengths were observed in the **PA1** solution above the CMC (100 μM) at pH 5.5 and 7.5 (Figure S4). Conversely, not a clear nanostructure but only amorphous aggregate was observed for **PA2** either at pH 5.5 or 7.5 (data not shown). In PA design, introducing a β-sheet forming peptide represents an effective approach for self-assembly into one-dimensional structures through intramolecular hydrogen bonding along the long axis.[20,21] It is clear that the β-sheet structure of **PA1** plays an important role in self-assembling into well-defined nanofibers.

The membrane activity of the PAs was examined by monitoring the leakage of encapsulated calcein from egg PC (EPC) liposomes. PA was added to liposome suspensions containing 100 μM EPC with various PA:EPC ratios. The released calcein increased in proportion to the PA:EPC ratio and **PA2** showed higher permeation activity than **PA1** both at pH 5.5 and 7.5 (Figure 2). The amphipathic nature of the GALA-based α-helix was shown to be important for the membrane permeation activity.[5] It is clear that the formation of an amphipathic α-helix by **PA2** is responsible for its membrane permeation activity. The tryptophan residue in the **PA2** sequence may have an additional effect on the permeation of membranes.[24,25] Although calcein leakage reached >90% in the presence of **PA2** with the PA:EPC ratio of 1:100 for pH 5.5 and 4:100 for pH 7.5, the leakage reached a plateau at ~25% for **PA1** with a ratio of 1:100 at pH 5.5 and at ~10% with the ratio of 4:100 at pH 7.5. Suppression of membrane activity of **PA1** at higher PA concentrations may be caused by the formation of β-sheet structures and self-assembly of **PA1**.[26] The assembled **PA1** nanofibers may bind to liposomes, but the calcein release profiles suggest that not the aggregate but the monomeric PA leads to the perturbation of the bilayer. Unlike **PA1**, **PA2** forms no defined nanostructure and the membrane permeation activity continues to increase in proportion to the PA:EPC ratio.

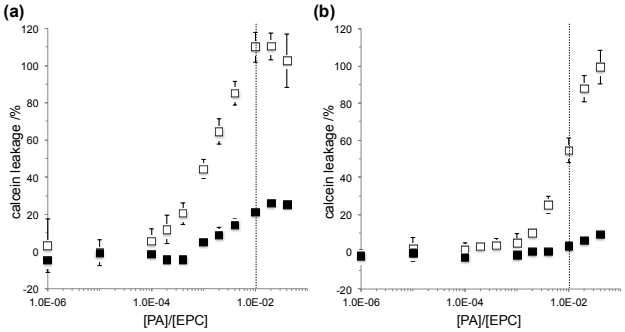

Figure 2. Liposomal leakage activities by **PA1** (filled square) or **PA2** (open square) at (a) pH 5.5 and (b) pH 7.5. Fluorescence intensities of released calcein were plotted against PA/EPC ratios. Data are mean ± SD from representative runs.

For both PAs, higher leakage of calcein was observed at pH 5.5 than pH 7.5. The pH responsive permeation of membranes by the GALA peptide is usually explained by the pH responsive α-helix formation.[5,17] The amphipathic nature of the α-helix formed at lower pH facilitates the fusion of the peptide with the membrane to form pores. Given that both **PA1** and **PA2** show little difference in secondary structures between pH 5.5 and 7.5, this suggests that the higher permeation activity at pH 5.5 may stem from the increase in hydrophobicity at the lower pH rather than the secondary structure. It was shown that PAs composed of the GALA peptide and a lauryl tail led to membrane rupture through a surfactant-like mechanism at physiological pH; but the PA leaked an encapsulated low-molecular-weight dye in a similar manner to that observed for the GALA peptide at pH 5.5.[19] To investigate the mechanism how PAs in this study interact with membranes, a dynamic light scattering measurement was performed on liposomal suspensions with or without PA treatment. The scattering light intensity is a function of size of colloidal particles and can be used to monitor the stability of liposomes. When a liposome was treated with Triton X-100, a well-known nonionic surfactant, at a final concentration of 0.1 wt%, the scattering intensity dramatically decreased, which results from a membrane lysis (Figure S4). On the other hand, upon addition of **PA1** or **PA2** with a PA:EPC ratio of 1:100, the surfactant-like lysis was suppressed and the scattering intensity was nominally preserved both at pH 5.5 and pH 7.5. It is noteworthy that liposomes treated with **PA2** scattered >95% intensity of the light even though >99% (pH 5.5) or ~55% (pH 7.5) of calcein was released from the liposome (Figure 2a, Table S1). This behavior suggests that the EPC liposome maintains its structure upon addition of **PA2**; however, the amphipathic α-helix creates pores within the membrane that release calcein over time. For **PA1**, a similar mechanism seems feasible at pH 5.5 because >95% intensity of light was detected while ~20% of calcein was released; however, the mechanism remains unclear at pH 7.5 when most of calcein (~98%) is kept inside liposomes. Based on those results, we concluded that the calcein leakage induced by **PA2** both at pH 5.5 and 7.5 or by **PA1** at pH 5.5 was not because of liposome bursts, but because calcein could pass through the membrane presumably through pores formed by the PAs. Although PAs in this study are composed of much shorter peptide sequences (8 and 14 amino acids for **PA1** and **PA2**, respectively) than GALA (30 amino acids), the fundamental nature of the interactions with membranes at pH 5.5 may not differ.

Finally, cytocompatibility of PAs was examined using Chinese Hamster Ovary (CHO) cells. CHO cells were incubated in the presence of PAs for 24 h and the cell proliferation was examined by the WST assay. Both PAs showed negligible cytotoxicity to CHO cells up to 60 μM (Figure 3). Although **PA2** showed a relatively high perturbation activity towards liposomes at physiological pH, the activity was only evidenced for simple synthetic liposomes and not generally for any biological membranes.

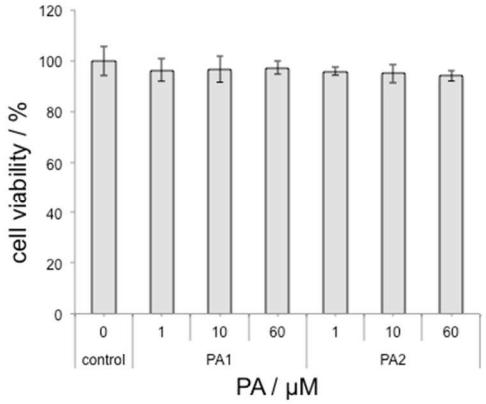

Figure 3. Cytotoxicity of PAs. Data are mean ± SD from representative runs.

Conclusions

In conclusion, we showed that PAs with peptide sequences of 2 or 3 repeating units of ALAE can act as pH-responsive membrane activators. **PA2** showed significantly higher membrane permeation activity than **PA1**, because **PA2** formed an amphipathic α-helix and did not self-assemble into a well-defined nanostructure. Our results provide a more productive way of using GALA-related peptides because the molecular design is more versatile and synthetically accessible. The efficacy of PAs when incorporated in a drug delivery carrier is currently ongoing in our laboratory.

Acknowledgments

This work was supported by a Grant-in-Aid for Scientific Research (S) 24226019 from the Ministry of Education, Culture, Sports, Science, and Technology of Japan, and the Sasakawa Scientific Research Grant from the Japan Science Society. The authors thank Professors Nobuo Kimizuka and Masaaki Morikawa, and Ms. Natsuko Ide for the facility support for the TEM measurement.

Notes and references

‡ Department of Applied Chemistry, Graduate School of Engineering, Kyushu University, Motooka 744, Nishi-ku, Fukuoka 819-0395, Japan
§ Center for Future Chemistry, Kyushu University, Motooka 744, Nishi-ku, Fukuoka 819-0395, Japan
¶ Center for Transdermal Drug Delivery, Kyushu University, Motooka 744, Nishi-ku, Fukuoka 819-0395, Japan
*E-mail: m-goto@mail.cstm.kyushu-u.ac.jp, phone: +81 92-802-2806, fax: +81-802-2810

†Electronic Supplementary Information (ESI) available: Materials, methods, and supplementary figures. This material is available free of charge via the Internet at http://pubs.acs.org. See DOI: 10.1039/c000000x/

1 J. M. White, *Annu. Rev. Physiol.,* 1990, **52**, 675.
2 R. Jahn, T. Lang and T. C. Südhof, *Cell,* 2003, **112**, 519.

3 W. Wickner and R. Schekman, *Nat. Struc. Mol. Biol.,* 2008, **15**, 658.
4 B. Gupta, T. S. Levchenko and V. P. Torchilin, *Adv. Drug Deliv. Rev.,* 2005, **57**, 637.
5 N. K. Subbarao, R. A. Parente, F. C. Szoka, L. Nadasdi and K. Pongracz. *Biochemistry,* 1987, **26**, 2964.
6 W. Li, F. Nicol and F. C. Szoka Jr., *Adv. Drug Deliv. Rev.,* 2004, **56**, 967.
7 T. Kakudo, S. Chaki, S. Futaki, I. Nakase, K. Akaji, T. Kawakami, K. Maruyama, H. Kamiya and H. Harashima, *Biochemistry,* 2004, **43**, 5618.
8 S. Futaki, Y. Masui, I. Nakase, Y. Sugiura, T. Nakamura, K. Kogure and H. Harashima, *J. Gene Med.,* 2005, **7**, 1450.
9 K. Sasaki, K. Kogure, S. Chaki, Y. Nakamura, R. Moriguchi, H. Hamada, R. Danav, K. Nagayama, S. Futaki and H. Harahima, *Anal. Bioanal. Chem.,* 2008, **391**, 2717.
10 Y. Sakurai, H. Hatakeyama, H. Akita, M. Oishi, Y. Nagasaki, S. Futaki and H. Harashima, *Biol. Pharm. Bull.,* 2009, **32**, 928.
11 S. Kobayashi, I. Nakase, N. Kawabata, H.–H. Yu, S. Pujals, M. Imanishi, E. Giralt and S. Futaki, *Bioconjugate Chem.,* 2009, **20**, 953.
12 H. Hatakeyama, E. Ito, H. Akita, M. Oishi, Y. Nagasaki, S. Futaki and H. Harashima, *J. Controlled Release,* 2009, **139**, 127.
13 H. Akita, K. Kogure, R. Moriguchi, Y. Nakamura, T. Higashi, T. Nakamura, S. Serada, M. Fujimoto, T. Naka, S. Futaki and H. Harashima, *J. Controlled Release,* 2010, **143**, 311.
14 I. A. Khalil, Y. Hayashi, R. Mizuno and H. Harashima, *J. Controlled Release,* 2011, **156**, 374.
15 Y. Sakurai, H. Hatakeyama, Y. Sato, H. Akita, K. Takayama, S. Kobayashi, S. Futaki and H. Harashima, *Biomaterials,* 2011, **32**, 5733.
16 F. S. Nouri, X. Wang, M. Dorrani, Z. Karjoo and A. Hatefi, *Biomacromolecules,* 2013, **14**, 2033.
17 R. A. Parente, S. Nir and F. C. Szoka Jr., *J. Biol. Chem.,* 1988, **263**, 4724.
18 C. Puyal, L. Maurin, G. Miquel, A. Bienvenüe and J. Philippot, *Biochim. Biophys. Acta,* 1994, **1195**, 259.
19 B. F. Lin, D. Missirlis, D. V. Krogstad and M. Tirrell, *Biochemistry,* 2012, **51**, 4558.
20 J. D. Hartgerink, E. Beniash and S. I. Stupp, *Science,* 2001, **294**, 1684.
21 S. E. Paramonov, H.–W. Jun and J. D. Hartgerink, *J. Am. Chem. Soc.,* 2006, **128**, 7291.
22 T. Muraoka, H. Cui and S. I. Stupp, *J. Am. Chem. Soc.,* 2008, **130**, 2946.
23 K. P. Ananthapadmanabhan, E. D. Goddard, N. J. Turro and P. L. Kuo, *Langmuir,* 1985, **1**, 352.
24 W.–M. Yau, W. C. Wimley, K. Gawrisch and S. H. White, *Biochemistry,* 1998, **37**, 14713.
25 M. R. R. de Planque, B. B. Bonev, J. A. A. Demmers, D. V. Greathouse, R. E. Koeppe II, F. Separovic, A. Watts and J. A. Killian, *Biochemistry,* 2003, **42**, 5341.
26 M. Rafalski, J. D. Lear and W. F. DeGrado, *Biochemistry,* 1990, **29**, 7917.

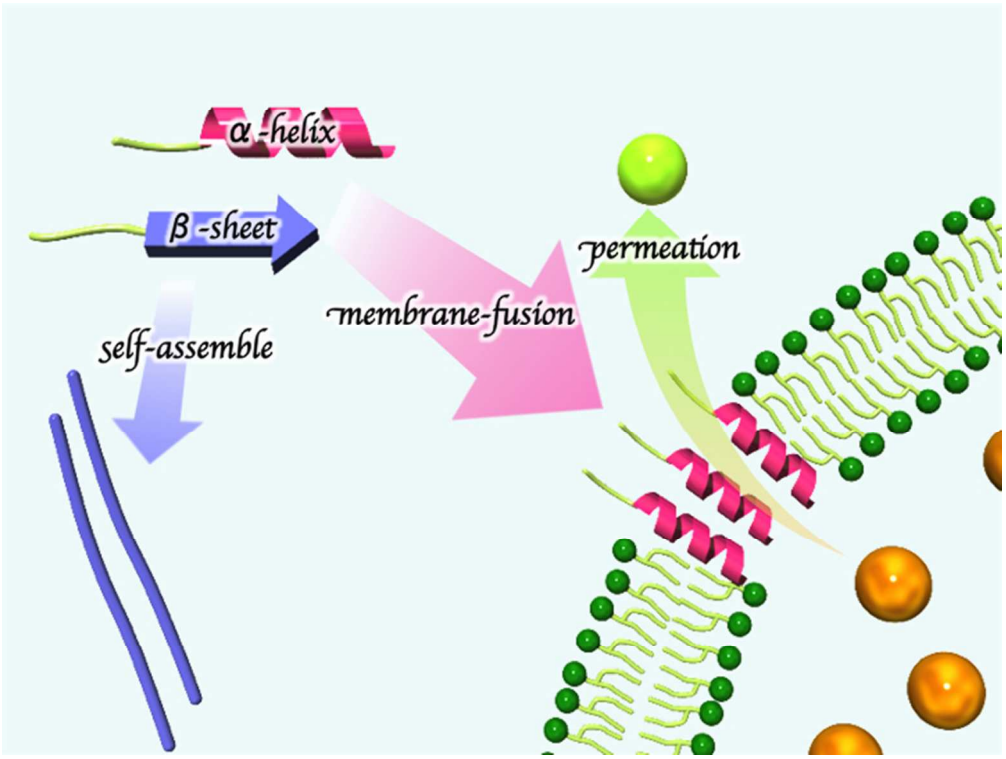

254x190mm (72 x 72 DPI)